Supporting Information: Mie 16-6 force field predicts viscosity with faster-than-exponential pressure dependence for 2,2,4-trimethylhexane

Richard A. Messerly

Thermodynamics Research Center, National Institute of Standards and Technology, Boulder, Colorado, 80305

Michelle C. Anderson

Thermodynamics Research Center, National Institute of Standards and Technology, Boulder, Colorado, 80305

S. Mostafa Razavi

Department of Chemical and Biomolecular Engineering, The University of Akron, Akron, Ohio, 44325-3906

J. Richard Elliott

Department of Chemical and Biomolecular Engineering, The University of Akron, Akron, Ohio, 44325-3906

SI.I. Input files

We provide example input files for simulating 2,2,4-trimethylhexane at 293 K with the Potoff force field in GROMACS (see attached .gro, .top, and .mdp files). Additionally, all files necessary to generate the results from this study can be found at www.github.com/ramess101/IFPSC_10.

Email addresses: richard.messerly@nist.gov (Richard A. Messerly), michelle.anderson@nist.gov (Michelle C. Anderson), sr87@zips.uakron.edu (S. Mostafa Razavi), elliot1@uakron.edu (J. Richard Elliott)

SI.II. MCMC from scoring function

Markov Chain Monte Carlo (MCMC) requires an expression for the likelihood function (L) and, in particular, the log (or natural log) of the likelihood function ($\ln(L)$). For example, by assuming a uniform prior in the model parameters and a symmetric proposal distribution, the Metropolis-Hastings acceptance criterion for an MCMC move only depends on L such that

$$\alpha = \frac{L(D|\theta_{\text{new}})}{L(D|\theta_{\text{old}})} \tag{1}$$

where D are the data, θ are the model parameters, and α is the probability of accepting a proposed or "new" parameter set (θ_{new}) given a previous or "old" parameter set (θ_{old}). For computational reasons, it is common to perform MCMC using the log-likelihood such that

$$\ln(\alpha) = \ln(L(D|\theta_{\text{new}})) - \ln(L(D|\theta_{\text{old}})) \tag{2}$$

By contrast, Mick et al. optimize the Potoff CH and C parameters using a scoring function (S) that weights the deviations for several different properties and their derivatives. This section describes how we translate the scoring function into a log-likelihood function, to then implement in MCMC.

SI.II.1. Derivation

Standard least squares minimization is mathematically equivalent to maximizing the likelihood function when assuming the errors follow a normal distribution. This can be readily verified from the following expression

$$\begin{aligned} L(D|\theta) = \prod_i \frac{1}{\sqrt{2\pi\sigma^2}} \exp\left[\frac{-1}{2\sigma^2}(y(\theta) - D_i)^2\right] = \frac{1}{\sqrt{2\pi^n\sigma^{2n}}} \exp\left[\frac{-1}{2\sigma^2}\left(\sum_i (y(\theta) - D_i)^2\right)\right] \\ = \frac{1}{\sqrt{2\pi^n\sigma^{2n}}} \exp\left(\frac{-SSE(\theta)}{2\sigma^2}\right) \end{aligned} \tag{3}$$

where n is the number of data points, σ is the standard deviation (which is assumed to be equal for all data points), $y(\theta)$ is the model estimate, and $\sum_i (y(\theta) - D_i)^2$ is the sum-squared-error (SSE). The log-likelihood can then be expressed as

$$\ln(L(D|\theta)) = \ln\left(\frac{1}{\sqrt{2\pi^n\sigma^{2n}}}\right) - \frac{SSE(\theta)}{2\sigma^2} \tag{4}$$

Substitution of Equation 4 into Equation 2 yields the MCMC acceptance probability

$$\ln(\alpha) = \frac{SSE(\theta_{\text{old}}) - SSE(\theta_{\text{new}})}{2\sigma^2} \tag{5}$$

note that the order of "new" and "old" changes due to the negative sign in Equation 4. Also, note the cancellation of the term in Equation 4 that does not depend on θ.

To this point, we have assumed that the standard deviation is constant with respect to the data. Relaxing this assumption, the likelihood is expressed as

$$\begin{aligned} L(D|\theta) = \prod_i \frac{1}{\sqrt{2\pi\sigma_i^2}} \exp\left[\frac{-1}{2\sigma_i^2}(y(\theta) - D_i)^2\right] &= C \exp\left[\sum_i \frac{-1}{2\sigma_i^2}(y(\theta) - D_i)^2\right] \\ &= C \exp\left[\sum_i -w_i(y(\theta) - D_i)^2\right] = C \exp\left(-WSSE(\theta)\right) \end{aligned} \tag{6}$$

where σ_i varies for D_i, C is a normalization constant equal to $\prod_i (2\pi\sigma_i^2)^{-1}$, and $WSSE$ is the weighted-sum-squared-error with weights (w_i) equal to σ_i^{-2}. The log-likelihood can then be expressed as

$$\ln(L(D|\theta)) = \ln(C) - WSSE(\theta) \tag{7}$$

and substitution into Equation 2 yields the MCMC acceptance probability for the weighted-sum-squared-error

$$\ln(\alpha) = WSSE(\theta_{\text{old}}) - WSSE(\theta_{\text{new}}) \tag{8}$$

Potoff's scoring function (S) is not simply the sum-squared-error or even the weighted-sum-squared-error. S is expressed in terms of the absolute percent deviation and each property is assigned a different weight that is not necessarily the inverse variance (σ_i^{-2}). Therefore, minimizing S is not equivalent to maximizing the likelihood of a normal distribution for neither constant nor varying σ. However, we can still apply the maximum likelihood criterion for Potoff's scoring function such that

$$L(D|\theta) = \prod_i C_i \exp\left(w_i \left|\frac{y(\theta) - D_i}{D_i}\right|\right) = C \exp\left(\sum_i w_i \left|\frac{y(\theta) - D_i}{D_i}\right|\right) = C \exp\left(-S(\theta)\right) \tag{9}$$

where C_i and C are normalization constants, and w_i are the weights assigned by Potoff (e.g.,

0.6135 for saturated liquid density, ρ_{liq}). Note that although Equation 9 utilizes an absolute percent deviation, rather than a weighted-sum-squared-error, the final expression is still analogous to Equation 6. Therefore, the log-likelihood for Potoff's scoring function is

$$\ln(L(D|\theta)) = \ln(C) - S(\theta) \tag{10}$$

and substitution into Equation 2 yields the MCMC acceptance probability for Potoff's scoring function

$$\ln(\alpha) = S(\theta_{\text{old}}) - S(\theta_{\text{new}}) \tag{11}$$

SI.II.2. Implementation

With Equation 11, all that remains to perform MCMC is a way to compute S for any θ. This is achieved by smoothing/interpolating the raw scoring function values (utilizing SciPy's RectBivariateSpline function in the interpolation sub-package[1]) over the two-dimensional grids of ϵ_{CH}-σ_{CH} and ϵ_{C}-σ_{C}. The values of S were obtained through private communication with Potoff's group. Only the scoring function values from the "long" CH and C parameters are utilized in this study. Using the "generalized" or "short" scoring function values would result in a different MCMC sampling of ϵ and σ.

The optimal "long" CH parameter is on the boundary of the grid tested by Mick et al. Therefore, we do not have any scoring function values from simulation for $\epsilon_{\text{CH}} < 14$ K. A similar problem is faced for $\epsilon_{\text{C}} < 0.8$ K and $\sigma_{\text{C}} > 0.63$ nm but, fortunately, these regions are rarely sampled by the MCMC algorithm. To overcome the challenge of extrapolating outside of the domain where $S(\theta)$ is available, we fit $\ln(S(\theta))$ to a multi-variate normal distribution. This approach works well for the CH parameters because the CH scoring function has a fairly normal shape. While the assumption of normality is worse for S over the ϵ_{C}-σ_{C} parameter space, this does not significantly affect our results because of the infrequent sampling of this extrapolation region.

[1] https://docs.scipy.org/doc/scipy/reference/generated/scipy.interpolate.RectBivariateSpline.html

SI.III. MCMC validation

This section validates the combined bootstrap re-sampling and MCMC approach. Specifically, we compare the uncertainties (depicted as histograms) obtained in two different manners. First, where a single replicate simulation is performed for each MCMC-nb parameter set, which are pooled together for bootstrap re-sampling ($N_{\text{reps}} = 1$, $N_{\text{MCMC}} = 40$). Second, where 40 replicate simulations are performed for each set of MCMC-nb parameters, and bootstrap re-sampling is performed independently for each set of 40 replicates ($N_{\text{reps}} = 40$, $N_{\text{MCMC}} = 30$). Due to the large amount of simulations required for this comparison, we perform this analysis on a simpler system, namely, ethane at 137 K and saturated liquid density using the Potoff force field.

Figure SI.1 demonstrates that the uncertainties are nearly indistinguishable for the two methods. This provides empirical evidence that performing a single simulation with each MCMC parameter set is the same as performing numerous simulations with each MCMC parameter set. Also of interest is that the numerical uncertainties ($N_{\text{reps}} = 40$, $N_{\text{MCMC}} = 1$) are much smaller than the overall uncertainties, suggesting that parameter uncertainties play a large role for ethane.

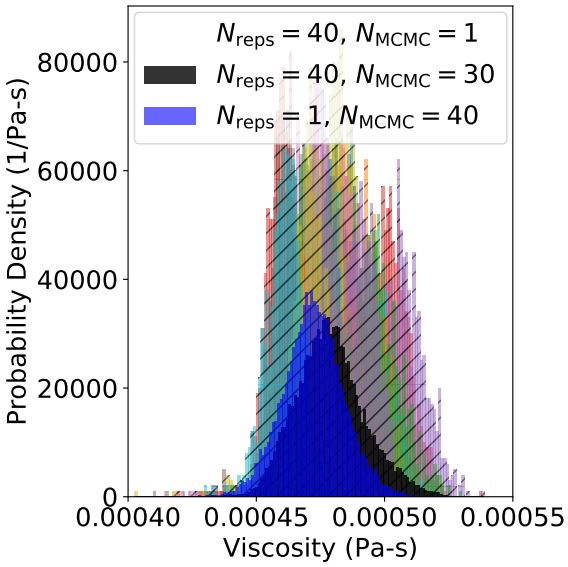

Figure SI.1: Validation of combined bootstrap re-sampling and MCMC approach utilized in study. Note that the uncertainties are almost indistinguishable between $N_{\text{reps}} = 1$, $N_{\text{MCMC}} = 40$ and $N_{\text{reps}} = 40$, $N_{\text{MCMC}} = 30$.

SI.IV. Torsion parameter uncertainty

In this section, we develop the skewed distribution for A_s, where the respective lower and upper 95 % confidence intervals correspond to -15 % and +40 % of the maximum torsional barrier. The viscosity values obtained with Potoff are considerably higher than those obtained with AUA4. Therefore, it is feasible, especially at higher pressures, that the optimal value of A_s is negative, i.e., the viscosity may be too high and, thus, decreasing the torsional barriers might improve the viscosity estimates. For this reason, unlike Nieto-Draghi et al., we consider $A_s < 0$.

To determine the appropriate scaling of the torsional barriers, Figure SI.2 presents a sensitivity analysis of η with respect to A_s. A_s is expressed as a percentage of the maximum for the non-shifted torsional potential. The viscosities in Figure SI.2 for 2,2,4-trimethylhexane are computed at 293 K and atmospheric pressure with 200 molecules and the Potoff force field. Also depicted is the only available experimental viscosity value at this temperature and pressure.

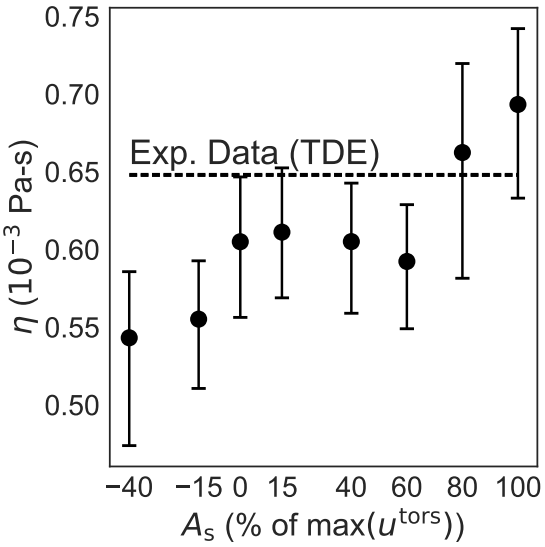

Figure SI.2: Sensitivity analysis of viscosity to torsional barrier heights. Simulations are performed at 293 K and atmospheric pressure. Experimental data are depicted as a dashed line. Uncertainties are expressed at 95 % confidence level, where the experimental uncertainty is approximately the line-width.

Figure SI.2 demonstrates that quantitative agreement with the experimental viscosity point necessitates an A_s value that is 80 % the maximum torsional barrier. Fearing some unforeseen consequences, we do not feel that obtaining quantitative agreement with this single experimental

value merits such a dramatic increase in the torsional barriers. For this reason, we adopt the largest percent increase proposed by Nieto-Draghi et al., i.e., 40 %.

By contrast, decreasing the torsional barriers by 40 % does have a significant impact on the predicted viscosity. We attribute this to the *gauche* barrier heights being approximately 40 % the *cis* barrier heights for the CH_i-CH_2-CH-CH_j torsional potential. Therefore, reducing all barriers by 40 % of the maximum torsional barrier nearly eliminates the equilibrium *gauche* conformations (see Figure 2 in the main text). Even a 15 % reduction has an appreciable effect on η. For this reason, we do not recommend reducing the barrier heights by more than 15 %.

SI.V. Tabulated MCMC parameter sets

Tables SI.I and SI.III provide tabulated values for the MCMC torsional and non-bonded parameter sets, respectively. Values are reported with the same precision as used in GROMACS .top files. Although 100 parameter sets are provided, only the first 60 were actually simulated.

Table SI.I: Tabulated torsional MCMC parameter sets, A_s/k_B (K).

CH_i-CH_2-CH-CH_j	CH_i-CH_2-C-CH_j
245.3217	366.2786
93.72992	-3.16439
490.0478	-2.58308
448.7307	-24.0214
428.2626	56.34298
590.7182	222.3622
-228.944	45.97479
253.95	27.81284
299.484	82.1421
243.3766	188.7071
513.7042	-39.7944
895.8756	134.1123
537.5786	45.97424
-182.423	18.25497
45.05584	85.61266
75.25501	197.7106
105.9541	57.97686
-43.7165	62.14353
436.2553	41.37991
-84.9937	55.6365
228.9903	56.12279
Continued on next page	

TABLE SI.I. – continued from previous page

CH_i-CH_2-CH-CH_j	CH_i-CH_2-C-CH_j
-79.5791	15.97303
474.2102	155.9151
106.9793	277.1976
334.8335	97.33988
-62.7642	7.885285
247.9064	310.0574
-158.449	18.91025
57.37419	-81.0976
178.6419	11.23948
154.0068	-5.22334
357.7532	197.1539
1030.707	115.1261
750.7104	181.558
369.7974	12.21172
407.7895	227.428
-30.0563	-48.886
218.0279	209.6781
271.6075	62.66278
471.0766	89.85051
-85.0217	49.63997
-13.1903	132.1259
81.33093	45.02805
117.5063	55.95632
53.04915	99.60283
215.6734	139.2832
-27.9557	-58.5935

Continued on next page

TABLE SI.I. – continued from previous page

CH_i-CH_2-CH-CH_j	CH_i-CH_2-C-CH_j
257.1062	106.205
520.3577	-94.2644
403.7061	206.9527
262.9882	79.38845
165.1618	220.6377
364.6917	338.5108
632.937	196.293
61.11979	138.1291
330.2237	15.64266
65.52998	51.72843
-17.544	50.3144
-2.54205	275.8895
-148.458	94.94305
33.35805	496.7659
434.5864	246.4159
17.58913	-6.24674
224.7114	347.9577
327.133	-141.765
31.14431	4.866992
235.5558	112.5681
63.15153	-103.184
36.59357	-47.5951
266.2478	-59.2604
-238.648	267.8193
45.25689	45.40068
417.7772	80.73735

Continued on next page

TABLE SI.I. – continued from previous page

CH_i-CH_2-CH-CH_j	CH_i-CH_2-C-CH_j
231.4378	118.4049
503.4451	-52.8715
220.9614	30.76672
-322.645	158.9019
600.3572	489.1167
584.0159	266.4777
378.0183	401.1579
-14.9356	233.7528
72.53771	116.0861
226.4172	75.67955
41.53055	281.8422
95.58026	-208.041
-103.085	-25.4343
168.2234	79.2551
198.6069	115.3935
188.2596	-36.8105
525.9425	133.5157
468.3856	311.4058
540.6453	103.8773
221.7239	63.60772
408.7145	54.53911
24.35917	10.04358
207.0636	252.9055
215.6001	99.484
188.4822	341.5431
48.54383	240.7821

Table SI.III: Tabulated non-bonded MCMC parameter sets. Note that the ϵ values are actually ϵ/k_{B}.

$\epsilon_{\mathrm{CH_3}}$ (K)	$\sigma_{\mathrm{CH_3}}$ (nm)	$\epsilon_{\mathrm{CH_2}}$ (K)	$\sigma_{\mathrm{CH_2}}$ (nm)	ϵ_{CH} (K)	σ_{CH} (nm)	ϵ_{C} (K)	σ_{C} (nm)
121.2209	0.37843	60.93017	0.398141	14.26033	0.471176	0.722454	0.609856
121.1843	0.378391	60.70465	0.398858	14.98545	0.454241	0.972753	0.614704
120.42	0.377758	61.36209	0.396935	14.86048	0.458331	1.134133	0.615871
121.2051	0.378086	61.21054	0.397999	13.72795	0.472212	1.320957	0.621433
120.8281	0.377928	61.02336	0.398455	14.03987	0.474321	1.081092	0.609649
120.9321	0.378008	61.63034	0.399088	13.28599	0.471348	1.250425	0.619892
120.5908	0.378036	61.21148	0.397336	13.84938	0.478092	1.053966	0.615041
120.3497	0.377624	61.41918	0.399439	13.81713	0.468061	0.950202	0.614273
120.8138	0.377977	61.43653	0.398538	14.53929	0.457495	0.993498	0.611464
120.7935	0.37803	60.99549	0.398378	14.3763	0.470453	1.249131	0.618245
120.9223	0.378054	60.99138	0.396732	15.10313	0.458056	1.311651	0.62049
120.3477	0.377869	61.54214	0.397295	12.11472	0.486955	0.906337	0.605561
120.8597	0.377868	61.17534	0.397263	13.71572	0.475002	0.84915	0.605687
120.9808	0.377992	61.48609	0.398934	14.73138	0.461487	1.192345	0.616653
120.633	0.377795	61.34852	0.396983	13.69362	0.480065	1.198975	0.622897
120.9178	0.377531	61.40116	0.39835	14.52292	0.469622	1.220123	0.619005
121.2373	0.377907	61.556	0.398192	14.02518	0.470341	1.141765	0.614652
121.1223	0.378028	61.08535	0.397717	13.81011	0.475105	0.931257	0.61701
120.9883	0.377696	60.87223	0.39807	14.28998	0.453893	1.035637	0.614
120.5882	0.377783	61.30355	0.397206	14.28375	0.472482	1.14147	0.626083
120.8989	0.377616	61.21552	0.396432	14.04822	0.465727	1.094789	0.615851
120.6549	0.377703	61.00533	0.395886	14.49659	0.46138	0.922215	0.602881
121.0036	0.377674	60.95302	0.397471	13.80565	0.475025	1.231178	0.616068
120.8221	0.377973	61.45514	0.398439	13.45654	0.476923	1.499958	0.623188
120.8922	0.378011	61.02064	0.39772	14.56367	0.464405	1.0542	0.614256

Continued on next page

TABLE SI.II. – continued from previous page

ϵ_{CH_3} (K)	σ_{CH_3} (nm)	ϵ_{CH_2} (K)	σ_{CH_2} (nm)	ϵ_{CH} (K)	σ_{CH} (nm)	ϵ_{C} (K)	σ_{C} (nm)
120.6293	0.37774	61.0676	0.397788	13.44343	0.469627	1.149418	0.616697
120.6077	0.377769	61.20697	0.396607	13.74279	0.471403	1.000763	0.609253
120.7359	0.378055	60.90119	0.398049	12.07802	0.477249	1.064561	0.607111
121.3054	0.377709	61.19525	0.396633	14.58498	0.465925	1.066605	0.618833
120.8334	0.377782	61.04248	0.396911	14.76422	0.457682	1.119002	0.617574
120.9144	0.378211	61.24366	0.398075	15.81163	0.453279	1.625457	0.626401
120.8947	0.378728	61.43469	0.397422	13.32113	0.47061	0.946886	0.617579
120.884	0.37784	60.99575	0.396429	13.77846	0.476656	1.200543	0.621941
120.8125	0.377846	61.07626	0.398664	13.15378	0.473225	1.151238	0.616479
121.2011	0.378244	61.33906	0.399486	13.3799	0.481115	1.122794	0.615556
120.5314	0.378117	61.3784	0.398285	13.60344	0.480496	1.13501	0.621474
120.5632	0.378054	61.43523	0.396348	14.98649	0.4583	0.947847	0.608811
120.3	0.377539	61.22244	0.398801	13.99417	0.468562	1.424783	0.624723
120.5889	0.378194	61.11738	0.397983	13.91949	0.469009	0.899078	0.611253
121.0962	0.378149	62.02168	0.39892	13.3353	0.47444	0.815328	0.599909
120.7433	0.377743	61.372	0.398694	14.09533	0.480547	1.176575	0.615112
121.2465	0.377925	61.46548	0.398494	15.61606	0.454104	1.117592	0.616507
120.8316	0.377693	60.94344	0.398394	14.44297	0.471578	1.241637	0.617563
120.7248	0.378095	61.2398	0.396768	12.80725	0.478474	1.205923	0.615929
120.5409	0.378047	61.78839	0.398008	13.33792	0.472624	1.51526	0.62572
120.5245	0.377436	61.48361	0.398735	14.75721	0.464541	0.936981	0.61
120.8378	0.378413	61.43264	0.397382	14.09467	0.466736	0.917496	0.615451
120.6077	0.377769	61.32968	0.396326	14.98649	0.454375	0.846744	0.610656
120.8013	0.377685	61.08185	0.399149	14.02211	0.470295	1.228272	0.616004
120.8002	0.378038	61.24112	0.397205	14.69626	0.464812	1.333836	0.619446
120.8702	0.377716	61.19626	0.398989	14.2943	0.466487	1.008621	0.613626

Continued on next page

TABLE SI.II. – continued from previous page

ϵ_{CH_3} (K)	σ_{CH_3} (nm)	ϵ_{CH_2} (K)	σ_{CH_2} (nm)	ϵ_{CH} (K)	σ_{CH} (nm)	ϵ_{C} (K)	σ_{C} (nm)
120.5566	0.377563	61.1238	0.397159	14.50663	0.472435	1.587145	0.634298
120.7546	0.377712	60.90201	0.397799	14.40579	0.45522	0.842027	0.602276
121.1835	0.378089	61.2142	0.399084	14.46465	0.457694	1.016685	0.612288
120.4242	0.377524	61.0022	0.39824	14.18673	0.464603	1.1123	0.61648
120.6992	0.378018	61.43452	0.398778	15.53899	0.447584	0.816128	0.600419
120.8565	0.378068	61.12153	0.398138	13.29391	0.47663	1.730034	0.627304
120.9195	0.378003	61.41236	0.398283	14.56452	0.462646	1.006147	0.616848
120.9391	0.377728	61.19499	0.398681	14.33341	0.462532	1.22465	0.61705
120.5281	0.378009	61.08732	0.396957	12.85624	0.487019	1.403197	0.622519
120.7392	0.377891	61.28535	0.399061	13.71831	0.477755	1.198656	0.616449
120.3477	0.377869	61.21984	0.399147	15.41724	0.445934	1.081185	0.613982
120.873	0.378029	61.24275	0.397367	13.54309	0.475461	1.12253	0.622381
120.9174	0.378277	60.99199	0.39622	13.62989	0.477038	1.317569	0.624603
121.1164	0.377827	61.35811	0.400252	15.49662	0.456112	0.935494	0.614305
120.5659	0.378031	61.11422	0.398279	14.27381	0.467172	1.18618	0.6124
121.0304	0.377769	60.5326	0.398241	13.51585	0.475263	0.81179	0.596633
120.783	0.377701	60.70465	0.398858	13.19274	0.475498	1.173788	0.620114
121.0872	0.378121	61.41019	0.399234	15.94324	0.448806	1.031287	0.616815
120.4257	0.378161	61.02356	0.397577	14.92078	0.469759	1.083418	0.617548
120.493	0.377966	61.24516	0.39791	13.29373	0.47108	1.10433	0.614309
120.9793	0.378326	61.39541	0.397383	13.99322	0.473327	1.003301	0.611422
120.6477	0.377887	61.41084	0.399321	15.29587	0.459907	1.044848	0.611587
120.9574	0.377844	61.59412	0.398838	13.94693	0.462676	0.839454	0.600877
120.7668	0.378017	60.86786	0.395478	15.79674	0.459803	1.232453	0.622071
120.9392	0.377601	61.49305	0.398502	12.74683	0.477507	1.315585	0.619615
120.4491	0.377956	61.07897	0.397959	14.94057	0.458613	0.858513	0.615574

Continued on next page

TABLE SI.II. – continued from previous page

ϵ_{CH_3} (K)	σ_{CH_3} (nm)	ϵ_{CH_2} (K)	σ_{CH_2} (nm)	ϵ_{CH} (K)	σ_{CH} (nm)	ϵ_{C} (K)	σ_{C} (nm)
120.907	0.378164	61.12295	0.397008	14.03987	0.474321	1.413469	0.617989
120.9422	0.378098	60.77126	0.396911	13.69009	0.474988	1.111536	0.616533
120.7685	0.378202	61.41013	0.397047	14.26239	0.464984	1.184975	0.61446
120.7486	0.378069	60.8793	0.397782	13.29237	0.482816	0.836705	0.599388
120.7021	0.37798	61.09967	0.396752	14.77505	0.459273	1.413156	0.620653
120.8423	0.377991	61.42776	0.396845	12.74553	0.477127	1.214702	0.615614
120.9605	0.378288	60.6915	0.398501	13.0965	0.478356	0.839722	0.591626
120.7579	0.378254	61.17535	0.397264	14.05405	0.467901	0.889036	0.613389
121.2533	0.378072	61.20622	0.398521	14.33572	0.476896	0.865138	0.609071
120.8302	0.378006	61.02781	0.398762	15.47468	0.457423	0.887533	0.601265
120.5137	0.378086	61.29736	0.399438	13.34752	0.474966	1.170867	0.62078
120.9641	0.378172	61.60907	0.396696	13.86355	0.476692	1.042944	0.607447
120.5281	0.378351	61.29425	0.397032	13.88876	0.46657	1.195816	0.612639
120.7391	0.3783	61.63098	0.397137	13.49024	0.473777	1.10932	0.619448
120.4928	0.378031	60.7591	0.397451	14.8615	0.467614	1.03509	0.613726
120.424	0.377537	61.25674	0.398287	13.34924	0.476028	1.366871	0.61924
120.8467	0.378151	61.28298	0.397136	13.78907	0.47335	0.900885	0.603027
121.0189	0.377927	61.21691	0.398272	13.49826	0.478881	1.069788	0.617952
120.8719	0.37822	61.63054	0.399191	14.76964	0.45586	1.263937	0.618749
121.0685	0.37805	61.21881	0.398669	13.28437	0.481424	1.307178	0.60968
120.5889	0.378194	61.08082	0.397661	13.44874	0.471396	0.968469	0.610344
120.8765	0.378457	60.92611	0.396805	14.55612	0.4693	1.17923	0.621328

SI.VI. Green-Kubo integrals

Figure SI.3 presents the average Green-Kubo integral for all thirteen state points. Note that much longer simulations are required for high pressures/viscosities (bottom panel) than for low pressure/viscosities (top panel).

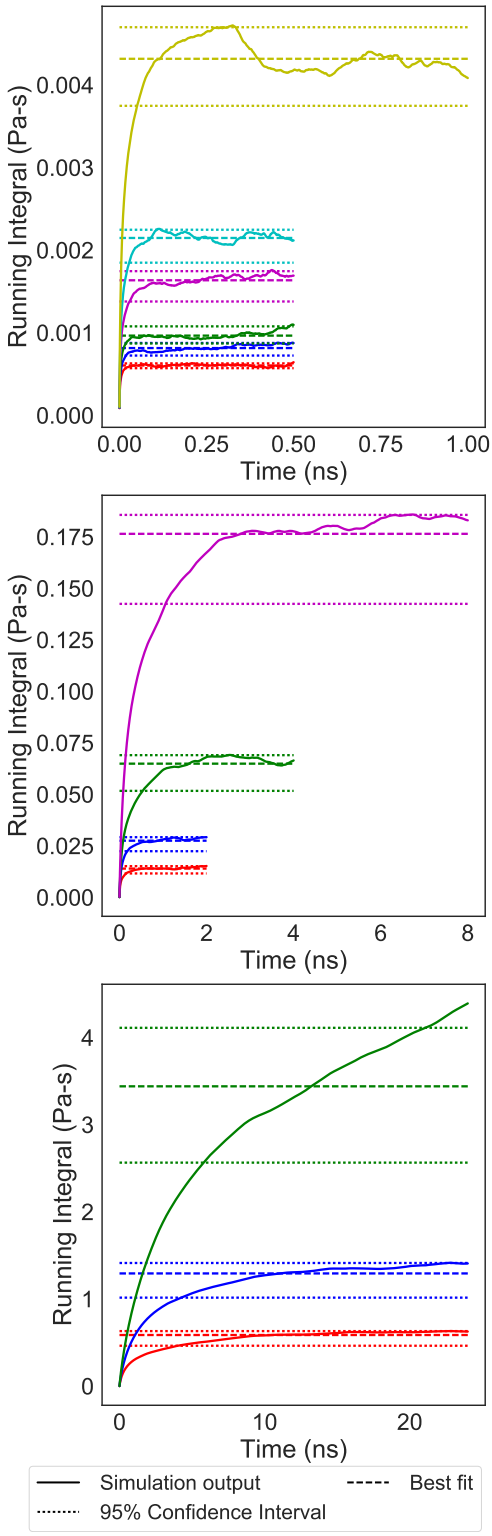

Figure SI.3: Green-Kubo integrals with respect to time. Top, middle, and bottom panels depict, respectively, low, intermediate, and high pressure/viscosity simulations where respective simulation times of 1 to 4 ns, 8 to 16 ns, and 24 to 48 ns are required to observe a Green-Kubo plateau.

SI.VII. Output frequency

Figure SI.4 presents the average Green-Kubo integral for different output frequencies.

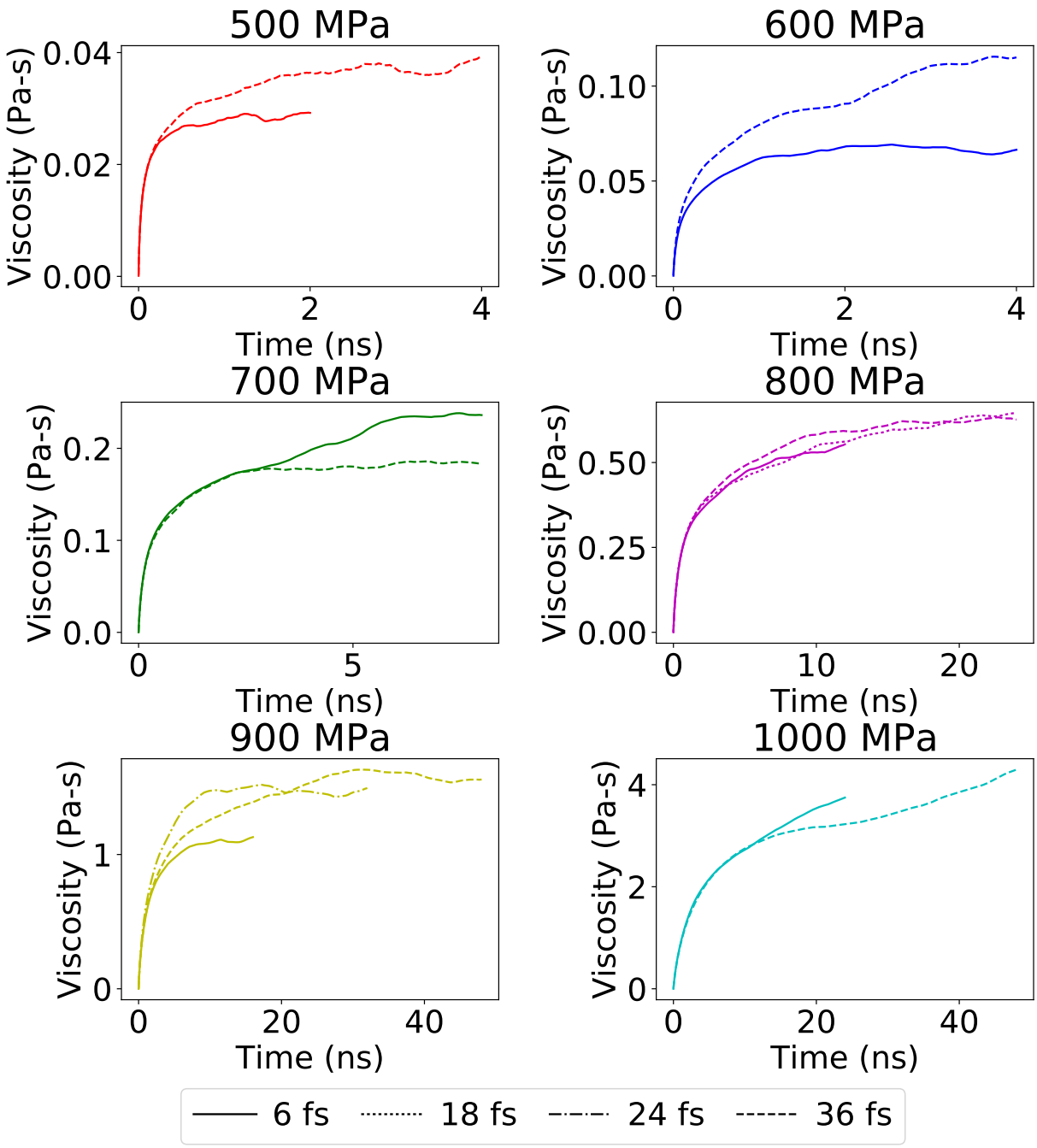

Figure SI.4: Comparison of different output frequencies for highest pressure simulations.